Editors' Suggestion | Featured in Physics

Experimental Test of the Edwards Volume Ensemble for Tapped Granular Packings

Ye Yuan,[1] Yi Xing,[1] Jie Zheng,[1] Zhifeng Li,[1] Houfei Yuan,[1] Shuyang Zhang,[1] Zhikun Zeng,[1] Chengjie Xia,[2] Hua Tong,[1,3] Walter Kob,[1,4] Jie Zhang,[1,5] and Yujie Wang[1,6,*]

[1]*School of Physics and Astronomy, Shanghai Jiao Tong University, Shanghai 200240, China*
[2]*School of Physics and Electronic Science, East China Normal University, Shanghai 200241, China*
[3]*Department of Physics, University of Science and Technology of China, Hefei 230026, China*
[4]*Laboratoire Charles Coulomb, UMR 5521, University of Montpellier and CNRS, 34095 Montpellier, France*
[5]*Institute of Natural Sciences, Shanghai Jiao Tong University, Shanghai 200240, China*
[6]*Materials Genome Initiative Center, Shanghai Jiao Tong University, Shanghai 200240, China*

(Received 12 March 2021; accepted 14 May 2021; published 28 June 2021)

Using x-ray tomography, we experimentally investigate granular packings subject to mechanical tapping for three types of beads with different friction coefficients. We validate the Edwards volume ensemble in these three-dimensional granular systems and establish a granular version of thermodynamic zeroth law. Within the Edwards framework, we also explicitly clarify how friction influences granular statistical mechanics by modifying the density of states, which allows us to determine the entropy as a function of packing fraction and friction. Additionally, we obtain a granular jamming phase diagram based on geometric coordination number and packing fraction.

DOI: 10.1103/PhysRevLett.127.018002

Granular packings are intrinsically nonequilibrium, as they stay in mechanically metastable configurations in the absence of external driving. However, when a granular system is subject to a specific excitation protocol like consecutive tapping, it can reach a stationary state whose packing fraction fluctuates around a specific value independent of the preparation history [1–5], reminiscent of a system in thermal equilibrium [6,7]. Edwards and coworkers proposed a statistical mechanics approach to account for this observation, postulating that for granular systems volume is the quantity which is analogous to energy for systems in thermal equilibrium [7–9]. In this approach, the corresponding conjugate to volume is a temperaturelike variable called "compactivity," which describes the compaction capability for a granular system. This framework was later extended to include contact forces in a jammed configuration which introduces the force or stress ensemble [10,11], although its relationship with the volume ensemble remains debated [12–14].

The Edwards ensemble approach has been investigated by a number of experimental and numerical studies. It is found that when a granular assembly reaches the steady state, local quantities like volume [15–21] or stress [11,20,22] possess a Boltzmann-like distribution. Furthermore, a numerical study has shown that mechanically stable frictionless packings are equally probable at the jamming point, verifying Edwards' original conjecture that the logarithm of the number of mechanical stable packings gives granular entropy [23]. Other simulations have found that the Edwards compactivity equals the dynamic effective temperature in slowly driven granular materials, leading to a granular version of the fluctuation-dissipation theorem [24,25]. Establishing this connection is important since it proves the usefulness of thermodynamic framework for the development of a constitutive theory for granular materials [26,27].

Despite these advances, a systematic experimental verification of Edwards volume ensemble in three dimensions (3D) is still lacking. For example, it remains controversial whether or not compactivity defined over the volume ensemble satisfies the thermodynamic zeroth law [20]. Furthermore, previous experimental investigations mainly focused on a single species of granular beads, i.e., with the same friction coefficient. The explicit role friction plays on granular statistical mechanics remains thus little understood [28].

In this Letter, we address these unresolved issues by analyzing tapped granular packings in 3D using an x-ray tomography technique [5,15,29,30]. We employ three types of monodisperse beads with different friction coefficients. Our results support the validity of the Edwards volume ensemble and the existence of a thermodynamic zeroth law. Furthermore, we find that at a given volume, both the density of states and the entropy increase with friction, which elucidates the specific way that friction influences granular statistical mechanics. Additionally, we obtain a granular jamming phase diagram based on geometric coordination number and packing fraction, which sheds light on the potential coupling between the volume and stress ensembles.

We generate disordered granular packings via mechanical tapping for three types of monodisperse spherical beads

in a dry cylindrical container. We employ acrylonitrile butadiene styrene plastic (ABS) beads, 3D-printed (3DP) plastic beads (ProJet MJP 2500 Plus), and 3D-printed plastic beads that have a bumpy surface (BUMP). A BUMP particle is designed by decorating a sphere of diameter d with 100 semispheres of diameter $0.1d$ on its surface (see Supplemental Material [31]). Such BUMP beads mimic the particles with large surface friction while maintaining a geometrical shape almost identical to an ideal sphere [32]. The bead diameters are $d = 6$ mm for 3DP beads, and $d = 5$ mm for ABS and BUMP beads. Their effective friction coefficients follow $\mu_{\mathrm{BUMP}} > \mu_{\mathrm{3DP}} > \mu_{\mathrm{ABS}}$ as measured by repose angle measurements [31]. The inner diameter of the cylindrical container is $D = 140$ mm and the height of the packing is roughly 140–210 mm. We glue ABS semispheres with $d = 5$ and 8 mm on the bottom and side walls of the container to avoid crystallization of the packing during the whole compaction process.

A mechanical shaker is used to excite the granular packings, with tap intensity $\Gamma = 2g$–$16g$, where g is the gravitational acceleration constant. A tap cycle consists of a 200 ms pulse followed by a 1.5 s interval allowing the system to settle. We note that the pulse duration is an important control parameter for tapping [33], but for the sake of simplicity we focus here only on Γ, while keeping the pulse duration constant. The compaction process starts from an initial poured-in random packing structure. Depending on Γ, the numbers of taps needed to reach the stationary states are between 10 and 4000 [31]. In general, a stronger tap intensity leads to a looser stationary state packing. X-ray tomography scans are performed on the stationary state packings using a medical CT scanner (UEG Medical Group Ltd., 0.2 mm spatial resolution). Subsequently, 3D packing structures are obtained following image processing procedures of previous studies [5,34]. For the analysis presented here, each packing consists of 3000–6000 particles, after excluding particles within $2.5d$ from the container boundary and free surface. By means of the pair correlation function, the bond orientational order metrics [35], and the local packing profiles along both the vertical and radial directions, we verify that the obtained packings are homogeneously disordered [31]. Statistics for each stationary state are the average results over 10–30 independent realizations.

The global packing fraction ϕ is calculated using $\phi = \sum v_p / \sum v_{\mathrm{voro}}$, where v_p and v_{voro} are the particle volume and its associated Voronoi cell volume. For simplicity, we set in the following v_p as unity. As shown in Fig. 1(a), the relation between Γ and ϕ is not universal, i.e., ϕ depends not only on Γ but also on the friction coefficient μ: $\phi = 0.605$–0.640 for ABS, $\phi = 0.587$–0.640 for 3DP, and $\phi = 0.565$–0.625 for BUMP. The associated lower bounds are $\phi^* = 0.605$, 0.587, and 0.565. We have verified that ϕ^* can also be reproduced by a hopper

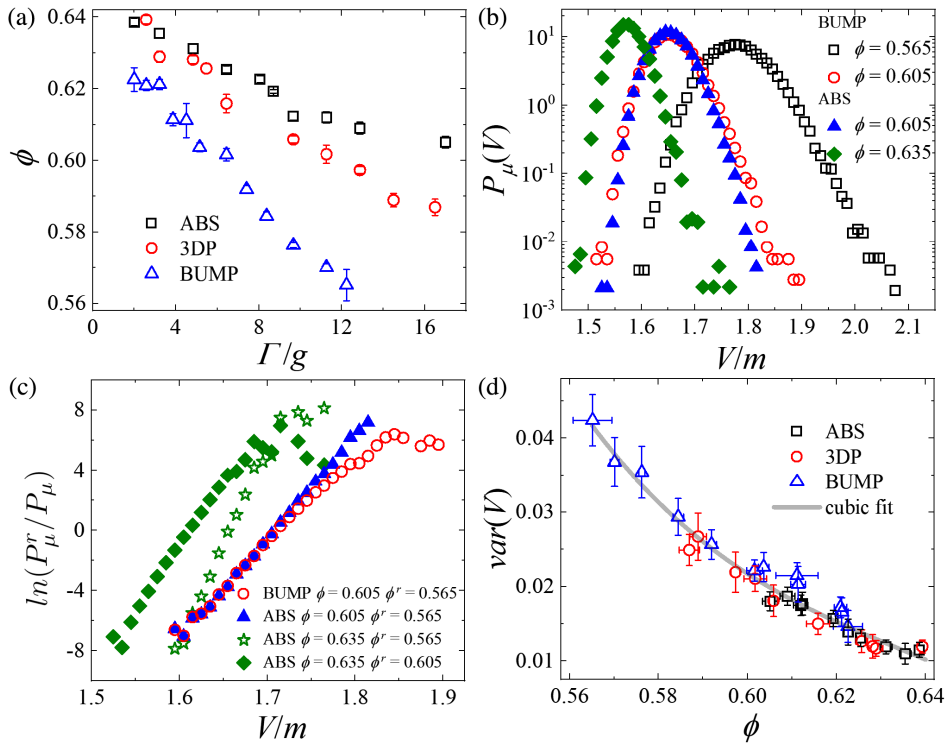

FIG. 1. (a) Packing fraction ϕ as a function of tap intensity Γ for the ABS, 3DP, and BUMP systems. (b) Probability distribution functions $P_\mu(V)$ for four representative packings. (c) Relationship between $\ln[P_\mu^r(V)/P_\mu(V)]$ and V/m for the packings shown in (b). (d) Volume fluctuation $\mathrm{var}(V)$ as a function of ϕ (symbols). The solid curve is a cubic polynomial fit (see main text).

deposition protocol, which is another typical way to generate very loose packings [31]. The independence of ϕ^* on the two protocols indicates that ϕ^* indeed marks the onset of mechanical stability for packings under gravity. Thus, the obtained ϕ range fully covers the range bounded between $\phi_{\mathrm{RLP}} \approx 0.56$ for the random loose packing (RLP) and $\phi_{\mathrm{RCP}} \approx 0.64$ for the random close packing (RCP) [5,30,36–39]. As we will demonstrate below, the significant overlaps of the ϕ range between different systems allow us to investigate systematically the role friction plays for the packings.

If the Edwards volume ensemble is valid in our system, compactivity should be an intensive quantity, whose value and the associated volume fluctuation should be independent of the system size. However, since the Voronoi volumes of neighboring particles are correlated, single-particle statistics cannot satisfy this requirement [21,40]. To avoid this issue, we calculate the total Voronoi volume V of particles within a coarse-grain spherical region of diameter $d(m/\phi)^{1/3}$ around each particle, where m is the number of particles within the sphere. In practice, we use $m = 15$, which is sufficient to suppresses the Voronoi volume correlations [31].

According to the Edwards volume ensemble, the probability of finding a system volume V is given by a Boltzmann-like distribution

$$P_\mu(V) = \frac{\Omega_\mu(V)}{Z_\mu(\chi)} e^{-V/\chi}, \tag{1}$$

where χ is the compactivity, $\Omega_\mu(V)$ is the density of states, $Z_\mu(\chi)$ is the partition function, and the subscript μ indicates the type of bead. In Fig. 1(b), we show the probability distribution function $P_\mu(V)$ for four representative packings. All these distributions can be fitted well by a k-Gamma function as previously reported [16], whose exponential tails are consistent with the Boltzmann-like distribution of Eq. (1). (We mention that with increasing m the distribution becomes Gaussian-like, as expected.) We note that $P_\mu(V)$ of ABS and BUMP at $\phi = 0.605$ are very similar to each other, indicating that $P_\mu(V)$ mainly depends on ϕ. Nevertheless, since $\Omega_\mu(V)$ depends on the type of bead considered, this similarity does not necessarily lead to a simple relation between χ and ϕ.

To measure χ, we use the overlapping histogram method which considers the ratio between $P_\mu(V)$ and $P^r_\mu(V)$ of a reference state with the same μ [9],

$$\frac{P^r_\mu(V)}{P_\mu(V)} = \frac{Z_\mu(\chi)}{Z_\mu(\chi^r)} e^{(1/\chi - 1/\chi^r)V}, \tag{2}$$

where χ^r is the compactivity of the reference state. In Fig. 1(c), the logarithm of the left hand side of Eq. (2) is plotted as a function of V/m for the configurations shown in Fig. 1(b) and the clear presence of linear regimes is recognized with the slopes corresponding to $(1/\chi - 1/\chi^r)m$. Hence, this allows us to determine χ if the reference state $P^r_\mu(V)$ and its χ^r can be identified. In analogy to the relation between the energy fluctuation and the specific heat in thermal equilibrium systems [5,9], χ can also be determined from the intensive volume fluctuation $\mathrm{var}(V) = \sigma_V^2/m$, where σ_V^2 is the variance of V. The associated relation is

$$\frac{1}{\chi(\phi)} - \frac{1}{\chi^r} = \int_{\phi^r}^{\phi} \frac{d\varphi}{\varphi^2 \mathrm{var}(V)}, \tag{3}$$

where ϕ^r is the packing fraction of the reference state. As shown in Fig. 1(d), surprisingly, $\mathrm{var}(V)$ for all three systems nearly collapse on a master curve, despite their rather different values of μ, in agreement with the $P_\mu(V)$ dependency on ϕ from Fig. 1(b). This master curve can be described well by a (phenomenological) cubic polynomial fit given by $\mathrm{var}(V) = 9.718 - 45.335\phi + 70.959\phi^2 - 37.225\phi^3$ [solid curve in Fig. 1(d)]. In previous work, the reference state (i.e., infinite χ) used in Eqs. (2) and (3) has often been chosen to be the RLP state with a fixed packing fraction $\phi_{\mathrm{RLP}} \approx 0.56$ [9]. Instead, we believe it is more suitable to define the infinite χ reference states as $\phi^r = \phi^* = 0.565$, 0.587, and 0.605 for BUMP, 3DP, and ABS, respectively, i.e., the loosest packing that can be obtained for a given μ [17]. The integral in Eq. (3) can be numerically calculated using the polynomial fit to $\mathrm{var}(V)$. Figure 2(a) shows that χ^{-1} calculated via Eq. (2) (symbols) are consistent with those via Eq. (3) (solid curves) for all three systems, which demonstrates the equivalency of the two methods [20,21]. The relationship between χ and ϕ for different systems [inset of Fig. 2(a)] qualitatively agrees with previous numerical studies [17,38]. The nice agreement of the probability distribution of V with the functional form of Eq. (1) and the consistency of results of two independent protocols to calculate χ therefore strongly support the validity of the Edwards volume ensemble in our system.

In Fig. 2(b), we observe a nice one-to-one correspondence between χ and tap intensity Γ for all three particle species within experimental uncertainty, where the margins of error are calculated assuming a 0.01 uncertainty for the values of ϕ^* in all three systems [31]. This result implies that two different granular packings (i.e., with different μ) under the same excitation intensity, i.e., same external heat bath, reach the same "temperature" (i.e., χ). Thus, a granular version of zeroth law of thermodynamics is fulfilled in our systems. Previous studies reported that two subsystems composed of two types of disks having different frictions reach different χ under quasistatic compression, over the whole ϕ range investigated [20]. This discrepancy with our conclusion might originate from the fact that quasistatic compression significantly hinders

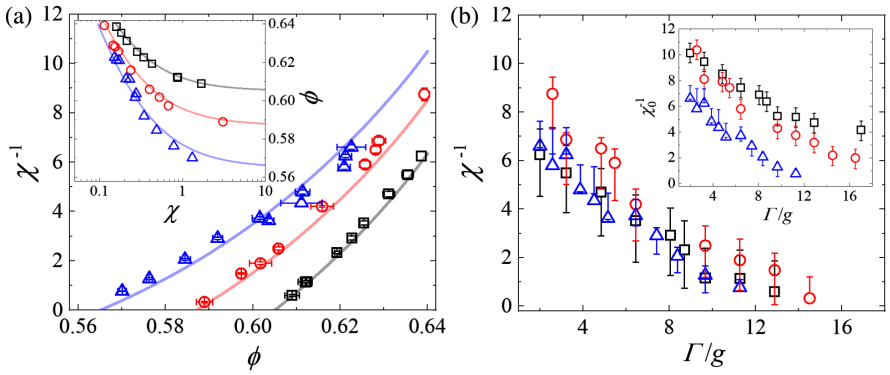

FIG. 2. (a) Inverse of compactivity χ^{-1} as a function of ϕ for the three systems calculated via the overlapping histogram method (symbols) and the fluctuation relation method (solid curves). Inset: ϕ as a function of χ. (b) Inverse of compactivity χ^{-1} as a function of tap intensity Γ. Inset: χ_0^{-1} as a function of Γ, where χ_0 is the compactivity calculated with a constant RLP reference with $\phi^r = 0.565$. Error bars are evaluated by calculating χ^{-1} using Eq. (3) with $\phi^r = \phi^* \pm 0.01$.

structural rearrangement, which hampers two subsystems to reach thermal equilibrium in the volume ensemble. A further possibility for this discrepancy originates from the different definitions of the reference state for infinite χ in the two studies. If the compactivity is calculated by Eq. (3) using a constant RLP reference with $\phi^r = 0.565$ for all three systems, it simply becomes a function of ϕ, since $\mathrm{var}(V)$ only depends on ϕ as shown in Fig. 1(d). In this case, the one-to-one correspondence between Γ and compactivity is lost [inset of Fig. 2(b)]. The emergence of a thermodynamic zeroth law for granular materials is quite striking given that the dissipative dynamics and microscopic structures of different systems under the same Γ are rather distinctive as indicated by the relation between χ and ϕ in the inset of Fig. 2(a).

So far, we have not discussed the details of how friction influences the statistical behavior of our system. According to Eq. (1), since $\Omega_\mu(V) = P_\mu(V)e^{V/\chi}Z_\mu(\chi)$, the V dependence of $\Omega_\mu(V)$ is given by the product $P_\mu(V)e^{V/\chi}$. So when plotting $P_\mu(V)e^{V/\chi}$ as a function of V for a given μ with different χ, the data should collapse onto a master curve after being scaled by a scaling factor. Figure 3(a) shows that this is indeed the case, which suggests that the functional form of Eq. (1) is valid. Additionally, since the scaling factor of $P_\mu(V)e^{V/\chi}$ at finite χ needed to collapse this product onto its $\chi \to \infty$ expression is the χ-dependent $Z_\mu(\chi)/Z_\mu(\infty)$, we can obtain $Z_\mu(\chi)$ up to a scaling constant $Z_\mu(\infty)$. Similarly, $\Omega_\mu(V)$ is the product of the normalized master probability distribution $P_\mu^{\chi\to\infty}(V)$ with $Z_\mu(\infty)$, i.e., $\Omega_\mu(V) = P_\mu^{\chi\to\infty}(V)Z_\mu(\infty)$. Thus, we can also obtain $\Omega_\mu(V)$ for all three systems up to the scaling constant $Z_\mu(\infty)$. A simple inspection of the master curve distributions for the three systems clearly shows that the density of states $\Omega_\mu(V)$ depends on μ.

Once we obtain $Z_\mu(\chi)/Z_\mu(\infty)$, we can then evaluate the free energy by $F = -\chi \ln[Z_\mu(\chi)]$ with an additive constant $\chi \ln[Z_\mu(\infty)]$. In Fig. 3(b), we show F as a function of χ^{-1} and this dependence can be fitted well by the functional form $F(\chi) + \chi \ln[Z_\mu(\infty)] = c_1 + c_2\chi^{c_3}$, where the values of the fit parameters are given in [31]. From F we can now obtain the entropy by $S = -\partial F/\partial\chi$ and also $S(\chi)$ will have an unknown additive constant $\ln[Z_\mu(\infty)]$. To determine this constant, we postulate that S_{RCP} is zero for all three systems from which $Z_\mu(\infty)$ can be determined. Previous studies have proposed that S_{RCP} is a finite constant [17]. However, its value does not qualitatively affect the discussion here. The resulting $S(\phi)$ are shown in Fig. 3(c) (symbols), in qualitative agreement with previous numerical simulations [17]. Complemental to this approach, entropy can also be measured using the fluctuation method [5]:

$$S(\phi) - S_{\mathrm{RCP}} = \int_\phi^{\phi_{\mathrm{RCP}}} \frac{d\varphi}{\varphi^2\chi(\varphi)}, \tag{4}$$

as indicated by the dashed curves in Fig. 3(c). The agreement of both approaches gives additional strong support for the validity of the Edwards statistical mechanics description of our system. For a given ϕ, the value of $S(\phi)$ increases with increasing μ, which is reasonable since a larger μ can stabilize more packings at a given ϕ. This can also be confirmed by explicitly calculating the density of states $\Omega_\mu(V)$ which can be obtained by multiplying the curves in Fig. 3(a) by the constant $Z_\mu(\infty)$, as shown in Fig. 3(d). This result agrees qualitatively with a recent experiment on 2D disk packings [28].

Based on the Edwards volume ensemble, a jamming phase diagram for frictional granular materials has been constructed using mean-field theory [38]. To construct the corresponding diagram for a real system, we determine the geometric coordination number z for all the experimental packings. The procedure to determine z is strictly identical for all packings to exclude the errors introduced by image processing [27,31]. In Fig. 4, we show the relation between z and ϕ for all three systems, together with our simulation results of packings at jamming onset with varying μ

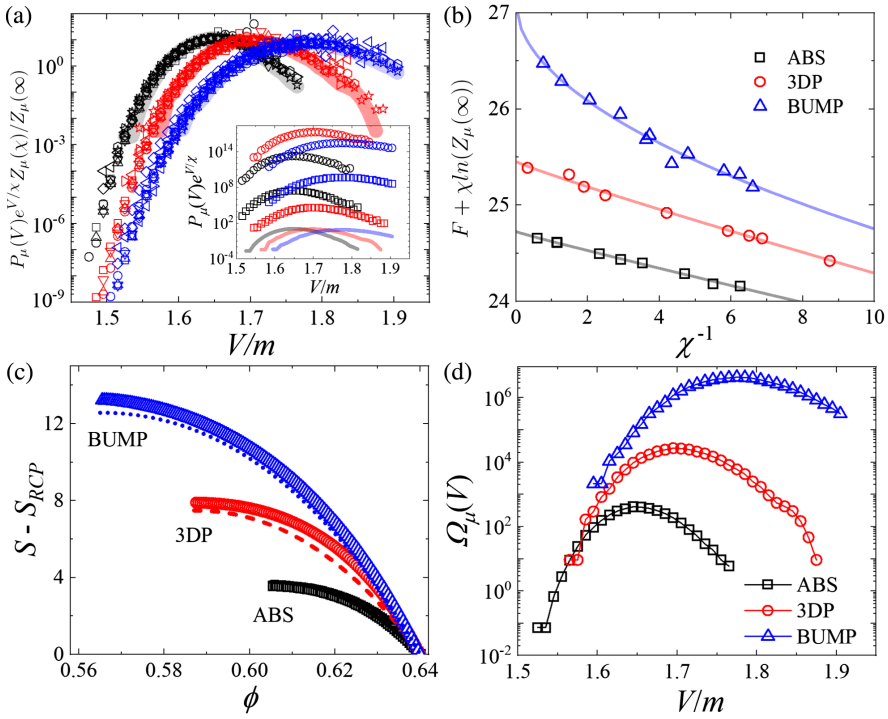

FIG. 3. (a) $P_\mu(V)e^{V/\chi}\,Z_\mu(\chi)/Z_\mu(\infty)$ as a function of V/m at different χ (different symbols) collapse on $P_\mu^{\chi\to\infty}(V)$ (thick solid curves) for the three systems. Inset: $P_\mu(V)e^{V/\chi}$ (symbols) at several χ for the three systems. Solid curves denote $P_\mu^{\chi\to\infty}(V)$. (b) $F+\chi\ln[Z_\mu(\infty)]$ as a function of χ^{-1} by experiments (symbols). Solid lines are fits (see main text). (c) S-$S_{\rm RCP}$ as a function of ϕ calculated via $S=-\partial F/\partial\chi$ (symbols) and the fluctuation relation method [Eq. (4), dashed curves], respectively. (d) Density of states $\Omega_\mu(V)$ as a function of V/m.

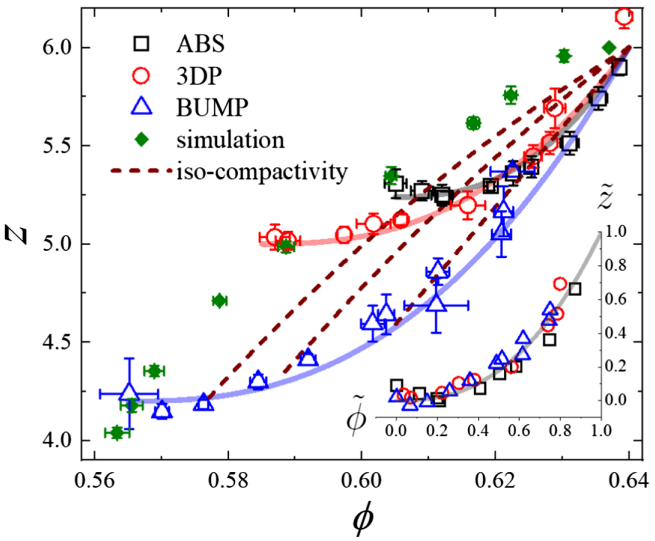

FIG. 4. Granular jamming phase diagram of coordination number z versus packing fraction ϕ from experimental measurements (open symbols) and simulation (filled diamonds). Dashed curves denote the isocompactivity lines for $\chi=0.8$, 0.4, and 0.2 (left to right). Inset: the relation between $\tilde{z}$ and $\tilde{\phi}$ (see main text) with an empirical fit $\tilde{z}=\tilde{\phi}^{2.5}$ (solid curve).

[31,41]. In contrast to the results of the mean-field calculation [38], we find that z is no longer just a function of ϕ, but shows a more complex behavior. For each system, we observe an onset (loosest) packing state with $z^*(\phi^*)$. $z^*=4.2$ for the loosest BUMP packings with $\phi^*=0.565$, which is close to the isostatic $z=4$ for the jamming transition as $\mu\to\infty$, i.e., RLP. For the other two systems we find that z^* increases with decreasing μ. Interestingly, $z^*(\phi^*)$ is rather close to our simulation results for frictional jamming onset, indicating a unique relation between z^*, ϕ^*, and μ. Beyond this onset state, for any of the systems, z grows with ϕ in a similar manner between the jamming onset and RCP. Introducing the scaled variables $\tilde{z}=(z-z^*)/(z^0-z^*)$ and $\tilde{\phi}=(\phi-\phi^*)/(\phi_{RCP}-\phi^*)$, where $z^0=6$ is the isostatic coordination number for RCP, we find that all three systems follow the empirical relation $\tilde{z}=\tilde{\phi}^{2.5}$, as shown in the inset of Fig. 4. For a given ϕ, the upper bound of z is formed by the corresponding onset $z^*(\phi^*)$, which reflects the geometrical constraint for a disordered hard-sphere configuration. At the same ϕ, $z(\phi,\mu)$ decreases with increasing μ, indicating that packings with a larger μ possess more mechanically stable configurations with small z. This result is thus different from previous study in which z only depends on ϕ and mechanically stable

configurations are instead related to the mechanical coordination number [38]. Our findings clearly suggest that z already encodes information about mechanical stability, which implies the coupling between the stress and volume ensembles for $\phi < \phi_{\mathrm{RCP}}$ [12].

Also included in Fig. 4 are isocompactivity lines (dashed curves) for $\chi = 0.8$, 0.4, and 0.2. The diagram of z and ϕ can then be transformed into another bivariate diagram of μ and χ, analogous to [38]. Note that a unique RCP state with $z^0 = 6$, $\phi \approx 0.64$ is approached as $\chi \to 0$, irrespective of μ. This convergence is also found in the behaviors of other structural parameters [31]. Therefore, geometric packing structure and its fluctuations at RCP are identical for systems with different μ, reinforcing the previous postulate that entropy S_{RCP} is constant at RCP for different systems, and stress and volume ensembles are decoupled at RCP [9].

In summary, by systematically studying tapped granular packings, we find strong evidence for the validity of the Edwards volume ensemble in 3D granular systems and establish a granular version of thermodynamic zeroth law. Additionally, we clarify how friction influences granular statistical mechanics as modifying the density of states. This allows us to determine the entropy as a function of packing fraction and friction, which will help to establish the connections between microscopic and macroscopic properties of granular materials. We believe these results are important since they show that the Edwards ensemble is indeed a coherent framework to describe the statistical properties of granular systems and it will help any future development of constitutive law of granular materials based on thermodynamic framework.

The work is supported by the National Natural Science Foundation of China (No. 11974240) and Shanghai Science and Technology Committee (No. 19XD1402100). W. K. is a member of the Institut Universitaire de France.

*Corresponding author.
yujiewang@sjtu.edu.cn

[1] E. R. Nowak, J. B. Knight, E. Ben-Naim, H. M. Jaeger, and S. R. Nagel, Density fluctuations in vibrated granular materials, Phys. Rev. E **57**, 1971 (1998).
[2] P. Philippe and D. Bideau, Compaction dynamics of a granular medium under vertical tapping, Europhys. Lett. **60**, 677 (2002).
[3] M. Schröter, D. I. Goldman, and H. L. Swinney, Stationary state volume fluctuations in a granular medium, Phys. Rev. E **71**, 030301(R) (2005).
[4] M. P. Ciamarra, A. Coniglio, and M. Nicodemi, Thermodynamics and Statistical Mechanics of Dense Granular Media, Phys. Rev. Lett. **97**, 158001 (2006).
[5] C. Xia, J. Li, Y. Cao, B. Kou, X. Xiao, K. Fezzaa, T. Xiao, and Y. Wang, The structural origin of the hard-sphere glass transition in granular packing, Nat. Commun. **6**, 8409 (2015).
[6] P. Richard, M. Nicodemi, R. Delannay, P. Ribiere, and D. Bideau, Slow relaxation and compaction of granular systems, Nat. Mater. **4**, 121 (2005).
[7] A. Baule, F. Morone, H. J. Herrmann, and H. A. Makse, Edwards statistical mechanics for jammed granular matter, Rev. Mod. Phys. **90**, 015006 (2018).
[8] S. F. Edwards and R. Oakeshott, Theory of powders, Physica (Amsterdam) **157A**, 1080 (1989).
[9] D. Bi, S. Henkes, K. E. Daniels, and B. Chakraborty, The statistical physics of athermal materials, Annu. Rev. Condens. Matter Phys. **6**, 63 (2015).
[10] R. C. Ball and R. Blumenfeld, Stress Field in Granular Systems: Loop Forces and Potential Formulation, Phys. Rev. Lett. **88**, 115505 (2002).
[11] S. Henkes, C. S. O'Hern, and B. Chakraborty, Entropy and Temperature of a Static Granular Assembly: An ab initio Approach, Phys. Rev. Lett. **99**, 038002 (2007).
[12] R. Blumenfeld, J. F. Jordan, and S. F. Edwards, Interdependence of the Volume and Stress Ensembles and Equipartition in Statistical Mechanics of Granular Systems, Phys. Rev. Lett. **109**, 238001 (2012).
[13] R. Blumenfeld, S. Amitai, J. F. Jordan, and R. Hihinashvili, Failure of the Volume Function in Granular Statistical Mechanics and an Alternative Formulation, Phys. Rev. Lett. **116**, 148001 (2016).
[14] K. Wang, C. Song, P. Wang, and H. A. Makse, Edwards thermodynamics of the jamming transition for frictionless packings: Ergodicity test and role of angoricity and compactivity, Phys. Rev. E **86**, 011305 (2012).
[15] T. Aste, Volume Fluctuations and Geometrical Constraints in Granular Packs, Phys. Rev. Lett. **96**, 018002 (2006).
[16] T. Aste and T. Di Matteo, Emergence of Gamma distributions in granular materials and packing models, Phys. Rev. E **77**, 021309 (2008).
[17] C. Briscoe, C. Song, P. Wang, and H. A. Makse, Entropy of Jammed Matter, Phys. Rev. Lett. **101**, 188001 (2008).
[18] S. McNamara, P. Richard, S. K. de Richter, G. Le Caër, and R. Delannay, Measurement of granular entropy, Phys. Rev. E **80**, 031301 (2009).
[19] T. Matsushima and R. Blumenfeld, Universal Structural Characteristics of Planar Granular Packs, Phys. Rev. Lett. **112**, 098003 (2014).
[20] J. G. Puckett and K. E. Daniels, Equilibrating Temperature-like Variables in Jammed Granular Subsystems, Phys. Rev. Lett. **110**, 058001 (2013).
[21] S.-C. Zhao and M. Schröter, Measuring the configurational temperature of a binary disc packing, Soft Matter **10**, 4208 (2014).
[22] E. S. Bililign, J. E. Kollmer, and K. E. Daniels, Protocol Dependence and State Variables in the Force-Moment Ensemble, Phys. Rev. Lett. **122**, 038001 (2019).
[23] S. Martiniani, K. J. Schrenk, K. Ramola, B. Chakraborty, and D. Frenkel, Numerical test of the Edwards conjecture shows that all packings are equally probable at jamming, Nat. Phys. **13**, 848 (2017).
[24] H. A. Makse and J. Kurchan, Testing the thermodynamic approach to granular matter with a numerical model of a decisive experiment, Nature (London) **415**, 614 (2002).

[25] A. Barrat, J. Kurchan, V. Loreto, and M. Sellitto, Edwards' Measures for Powders and Glasses, Phys. Rev. Lett. **85**, 5034 (2000).

[26] R. P. Behringer, D. Bi, B. Chakraborty, S. Henkes, and R. R. Hartley, Why Do Granular Materials Stiffen with Shear Rate? Test of Novel Stress-Based Statistics, Phys. Rev. Lett. **101**, 268301 (2008).

[27] Y. Xing, J. Zheng, J. Li, Y. Cao, W. Pan, J. Zhang, and Y. Wang, X-ray Tomography Investigation of Cyclically Sheared Granular Materials, Phys. Rev. Lett. **126**, 048002 (2021).

[28] X. Sun, W. Kob, R. Blumenfeld, H. Tong, Y. Wang, and J. Zhang, Friction-Controlled Entropy-Stability Competition in Granular Systems, Phys. Rev. Lett. **125**, 268005 (2020).

[29] B. Kou *et al.*, Granular materials flow like complex fluids, Nature (London) **551**, 360 (2017).

[30] C. Xia *et al.*, Origin of Noncubic Scaling Law in Disordered Granular Packing, Phys. Rev. Lett. **118**, 238002 (2017).

[31] See Supplemental Material at http://link.aps.org/supplemental/10.1103/PhysRevLett.127.018002 for details on experimental methods, additional packing characterizations, and simulation.

[32] S. Papanikolaou, C. S. O'Hern, and M. D. Shattuck, Isostaticity at Frictional Jamming, Phys. Rev. Lett. **110**, 198002 (2013).

[33] J. A. Dijksman and M. van Hecke, The role of tap duration for the steady-state density of vibrated granular media, Europhys. Lett. **88**, 44001 (2009).

[34] Y. Cao *et al.*, Structural and topological nature of plasticity in sheared granular materials, Nat. Commun. **9**, 2911 (2018).

[35] P. J. Steinhardt, D. R. Nelson, and M. Ronchetti, Bond-orientational order in liquids and glasses, Phys. Rev. B **28**, 784 (1983).

[36] G. Y. Onoda and E. G. Liniger, Random Loose Packings of Uniform Spheres and the Dilatancy Onset, Phys. Rev. Lett. **64**, 2727 (1990).

[37] M. Jerkins, M. Schröter, H. L. Swinney, T. J. Senden, M. Saadatfar, and T. Aste, Onset of Mechanical Stability in Random Packings of Frictional Spheres, Phys. Rev. Lett. **101**, 018301 (2008).

[38] C. Song, P. Wang, and H. A. Makse, A phase diagram for jammed matter, Nature (London) **453**, 629 (2008).

[39] L. E. Silbert, Jamming of frictional spheres and random loose packing, Soft Matter **6**, 2918 (2010).

[40] F. Lechenault, F. Da Cruz, O. Dauchot, and E. Bertin, Free volume distributions and compactivity measurement in a bidimensional granular packing, J. Stat. Mech. (2006) P07009.

[41] S. Plimpton, Fast parallel algorithms for short-range molecular dynamics, J. Comput. Phys. **117**, 1 (1995).